Elliptic Fourier Analysis on Female Chest Contour

Hui-Yao Zhang[1], Duan Li[1], Hao-Yang Xie[1], Yue-Qi Zhong[1,2*]

[1] *College of Textiles, Donghua University, Shanghai, 201620, China.*
[2] *Key Lab of Textile Science and Technology, Ministry of Education, Shanghai, 201620, China.*

*Corresponding author's email: zhyq@dhu.edu.cn

Abstract

In this paper, Elliptic Fourier Analysis (EFA) was used to study the chest shape of female subjects. Three kinds of sampling methods on chest contour analysis were first compared, including curvature sampling, random sampling and equally spaced sampling. According to the experiment, the equally spaced sampling is the best option. Secondly, the appropriate proper sampling density based on the mean distance and the chest circumference was discovered. Finally, the number of harmonics used by EFA was tested for acceptable error. The experimental results indicate that the EFA is an efficient method in female chest shape analysis.

Keywords: Elliptic Fourier Analysis; Sampling Method; Sampling Points; Harmonics

1. Introduction

Fourier transformation has been widely used in many engineering domains, especially, in signal analyzing and processing. Elliptic Fourier has been adopted to present the contour of image and analysis of object shape. In 1982, Kuhl [1] took Elliptic Fourier as the approach to describe closed contour curve. In biology field, Elliptic Fourier was used to describe object silhouette and Elliptic Fourier Descriptors (EFD) was used to measure shape differences [2-4]. For instance, Neto J C used EFDs to describe and analyze the shape of a plant leaf, and the coefficient of EFDs of the plant leaf was taken to identify the type of plant. Martin Friess [5] used Elliptic Fourier to research three dimensional curve forms and extract characteristic curves from human body scans. Then, the analyzing result was used to direct the design of the shape of the protective belt.

The shape and size of the human chest is one of the most important factors whenever a tailor measures a person for suitable clothing [6-8], or when a game engineer rebuilds a virtual body or a costume designer designs virtual [9] or real clothing. In the article, the female chest is selected as target since the male chest slice is easier to fit and reconstruct due to its simple contour.

In this paper, EFA was employed as the core approach to implement the whole study. According to the suggestions from several qualified tailors, a facile hypothesis was proposed that the number of sampling points is based on chest girth and maximum distance error, and mean error range is 1mm and 0.5mm respectively. Different number of sampling points of the same curve was selected to illustrate the huge differences of fitting effect. Next, several different sampling methods and sampling points with certain harmonics was taken to reconstruct the final fitting curve, where eight different models were used to testify the validity of our fitting.

2. Methodology

2.1 Data Collection

Kinnect was used to scan a female bust placed on a rotatable platform and the actual chest circumference was measured manually firstly. To make sure that the obtained data accuracy is sufficient, the environment is set to related standards. The temperature range is from 21 to 25 degree centigrade, and the humidity level is between 60% and 70%. After the human point cloud data was collected, the OBJ file was imported into GeoMagic Studio 12, a well-known professional engineering program brand of 3D system [10]. First, the holes was padded in the scanned model then the number of triangles was reduced for the purpose of computation efficiency. Next, the feature points was chosen manually before scanning, the model was cut horizontally and the chest curve was obtained. Lastly, several different discrete-closed curves was created with various sampling methods.

To testify the scanner accuracy, a cylinder was scanned. The diameter of the cylinder is 25cm and the height is 80cm. The scanned cylinder accuracy is analyzed. According to Fig.1, the scanning error increased from the center to both ends, and the scanning error got the maximum value which is less than 0.5cm, which could satisfy our experiment requirement.

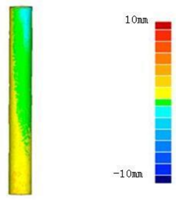

Fig.1 Testify the scanning system error with a cylinder

2.2 Elliptic Fourier Analysis

EFA was one of the most widely used tool for feature extraction and reconstruction of a single closed-curve. A continuous-closed curve could be considered as a continuous periodic function. According to the principle of Fourier Series, any periodic functions could be expressed by the sum of a series of sine and cosine functions with increasing frequencies. The coefficients of the Fourier Series were referred to as “Elliptic Fourier Descriptors” (EFDs) [6], which could be implemented to reconstruct the original shape with major features. EFDs was first proposed by [11] and the most significant reason for its popularity was that researchers can use it to represent all kinds of close contour meanwhile retaining the original information with limited number of coefficients. Moreover, it also provided robustness to translation, rotation and scale if the EFDs were normalized [12]. Lots of studies used EFDs to research, for example, the characteristics of animals and plants [13-16], anthropology [17], hand-written recognition [18] and aircraft contour description [19].

Suppose there are *K* discrete sampling points along a continuous-closed contour. This contour can be represented by a sequence of *x* and *y* coordinates which are ordered by counter-clockwise from an arbitrary starting point. The length from the starting point to the *p-th* point is denoted by t_p, and the perimeter of the whole contour is denoted by *T*, and $T = t_K$ where *K* is the total number of the discrete sampling points and Δt_i is the distance between the *(i-1)-th* point and *i-th* point. For each sampling point, the coordinates of *p-th* along x and y directions are:

$$t_p = \sum_{i=1}^{p} \Delta t_i \tag{1}$$

$$x_p = \sum_{i=1}^{p} \Delta x_i \tag{2}$$

$$y_p = \sum_{i=1}^{p} \Delta y_i \tag{3}$$

where Δx_i and Δy_i are the distance from *(i-1)-th* point to the *i-th* point along the *x* and *y* axes respectively. Thus, the Elliptic Fourier expansions of *x* and *y* coordinate along the contour are:

$$x_p = A_0 + \sum_{n=1}^{\infty} \left(a_n \cos\frac{2n\pi t_p}{T} + b_n \sin\frac{2n\pi t_p}{T}\right) \tag{4}$$

$$y_p = C_0 + \sum_{n=1}^{\infty}(c_n \cos\frac{2n\pi t_p}{T} + d_n \sin\frac{2n\pi t_p}{T}) \quad (5)$$

The coefficients a_n , b_n , c_n and d_n actually have the capacity to describe the outline of the original section and are known as Elliptic Fourier coefficient of the *n-th* harmonic. Notice that each harmonic is denoted by four Elliptic Fourier coefficients and the first harmonic is used to align the contour [19].

$$a_n = \frac{T}{2n^2\pi^2}\sum_{p=1}^{K}\frac{\Delta x_p}{\Delta t_p}\left(\cos\frac{2n\pi t_p}{T} - \cos\frac{2n\pi t_{p-1}}{T}\right) \quad (6)$$

$$b_n = \frac{T}{2n^2\pi^2}\sum_{p=1}^{K}\frac{\Delta x_p}{\Delta t_p}\left(\cos\frac{2n\pi t_p}{T} - \sin\frac{2n\pi t_{p-1}}{T}\right) \quad (7)$$

$$c_n = \frac{T}{2n^2\pi^2}\sum_{p=1}^{K}\frac{\Delta y_p}{\Delta t_p}\left(\cos\frac{2n\pi t_p}{T} - \cos\frac{2n\pi t_{p-1}}{T}\right) \quad (8)$$

$$d_n = \frac{T}{2n^2\pi^2}\sum_{p=1}^{K}\frac{\Delta y_p}{\Delta t_p}\left(\cos\frac{2n\pi t_p}{T} - \sin\frac{2n\pi t_{p-1}}{T}\right) \quad (9)$$

The equations above are the basic principles and tools that were used in this study. First, the Elliptic Fourier coefficient of *N* harmonics were computed according to sampling points, and then the fitting coordinates were computed based on the original sampling points.

2.3 Error Metrics

Four parameters were selected to measure the similarity of the original contour and fitting contour: 1) perimeter accuracy, 2) mean distance between original sampling points and fitting points, 3) standard deviation of distance between original sampling points and fitting points and 4) maximum distance between sampling points and reconstruction points.

1) Perimeter was treated as one of the error metrics since the number of sampling point is closely related to the contour perimeter, furthermore, the chest circumference is also a significant factor in garment industry.

Taking *O* as original/actual contour and *F* denoted as fitting contour. *P(O)* and *P(F)* are the perimeters of the original contour and the fitting contour, respectively. Then perimeter accuracy is computed as:

$$A = \frac{P(F)}{P(O)} \quad (10)$$

2) Mean distance ($\bar{D}$) reflects the deviation extent between the original shape and reconstruction shape. Mean distance is computed by the following formula where *K* is the total number of the sampling points.

$$\bar{D} = \frac{1}{K}\sum_{1}^{K} dist(O_i, F_i) i = 1, 2 \ldots K \quad (11)$$

3) The standard deviation of distance between original sampling points and fitting points (σ_D) reflects the measure variability which is computed as

$$\sigma_D = std(D_i) \tag{12}$$

4) The maximum distance between sampling points and fitting points is denoted as

$$D_{\max} = Max\{dist(O_i, F_i), i = 1, 2, ..., K\} \tag{13}$$

Now the core algorithm and the methods have been illustrated above as used to measure the errors. During the following sections all of the test results are based on them. Many related works focused on the field of image processing and there is no need to consider this problem because the pixels are naturally discrete [20].

3. Experimental Results and Discussion

3.1 Testing Sampling Methods

Three common sampling methods were included in this study, curvature sampling, random sampling and equally spaced sampling. In this step, these three kinds of sampling methods were used to obtain sampling points and the number of sampling point is equal. So 500 sampling points were selected per curve with different sampling methods and the number of harmonics is 15. Table 1 lists the result of the test. (All three discrete closed curve are created by GeoMagic Studio 12).

Table.1 Comparison of three different sampling methods with 500 discrete points and 15 harmonics

Error Metrics	Curvature Sampling	Random Sampling	Equally spaced Sampling
Mean Distance (mm)	5.56	6.78	0.87
Max Distance (mm)	7.82	8.63	1.72
Standard Deviation	24.39	28.46	0.42
Perimeter Accuracy	92.21%	98.01%	99.53%

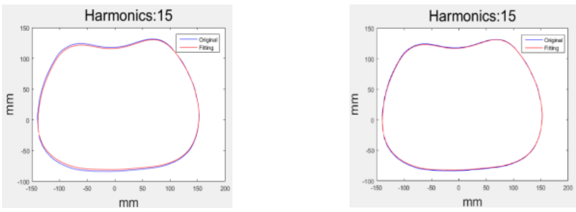

(a) curvature sampling (b) equally spaced sampling

Fig.2 (a) is the result of curvature sampling, at the left bottom corner, the gap between two contour was obvious. (b) is the result of equally spaced sampling. Both of them use 500 sampling points and 15 harmonics. White is the original contour and red is the fitting contour.

As shown in Table 1, the equally spaced sampling has the best performance. Curvature sampling and random sampling have the similar results but are far behind equally spaced sampling. So in the following sections equally spaced sampling was selected by default. Fig.2 (a) and (b) represent the fitting effects of curvature sampling and equally spaced sampling based on 500 sampling points and 15 harmonics.

The fitting effects of curvature sampling and equally spaced sampling

3.2 Sampling Density

The next step was to decide how many discrete points should be taken from the contour. Intuitively, the more points, the more accurate the results. However, the whole procedure would be time consuming if too many discrete points were selected. Conversely, if only a few number of points were employed, the preferable fitting result cannot be achieved even if higher harmonics were adopted. Fig.3 represents an extreme reconstruction example with 120 sampling points and 2000 harmonics. With more harmonics, more details will be kept. However, we cannot achieve the anticipated result with a few number of points in practice. Furthermore, the number of harmonics is constrained by the number of points along a contour, and the number of sampling points is corresponds to the length or size of the object. [21] Sanfilippo used 100 points corresponds with 43 harmonics to describe the shape of human laminas but without the explanation that why 100 sampling points are selected.

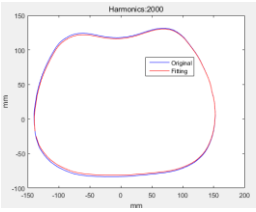

Fig.3 Construction result with 2000 harmonics and only 120 sampling points. The perimeter accuracy is 98.25%.

Intuitively, the number of points is closely related to the perimeter of a shape. This was also the reason why perimeter accuracy was chosen as one of the error metrics above. According to qualified tailors and garment designers' advice, for human measurement and the garment industry, 99% perimeter accuracy, 1mm maximum distance and 0.5mm mean distance can satisfy the practical requirements. Then, we proposed a facile hypothesis and verified the availability in the later section. The distance was used as the sampling interval of equally spaced sampling which means, for example, 0.5mm is the sampling interval so there will be 2000 sampling points if the girth of a closed curve is 100 cm.

3.3 Reconstruction with Limited Harmonics

For now, sampling method has been decided and the number of sampling points was also selected according to the perimeter of a contour. The only variable remaining was the number of harmonics, which was easy to decide according to the different fitting effects and error metrics. The chest circumference of the model was 840mm, so this chest contour could be divided into 1680 sampling points based on the hypothesis proposed in last section.

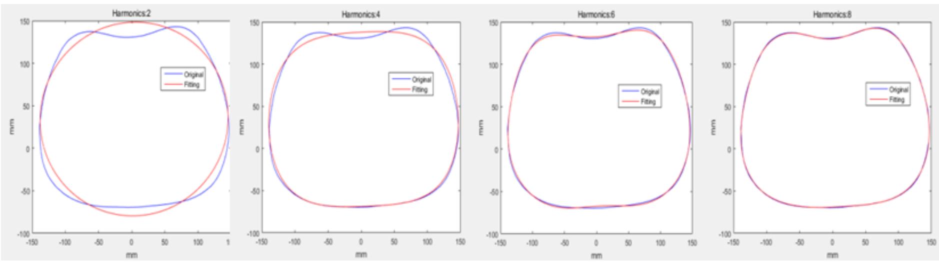

Fig.4 Four different results with the same 1680 discrete points and different harmonics.

Table 2. Errors of four different construction results.

It can be seen that after the number of sampling points was decided, the only thing needed to be done next is to test whether the number of harmonics could satisfy the acceptable errors.

Table.2 demonstrated the different imitations with the same number of sampling points with equally spaced sampling but different harmonics.

Harmonics	Perimeter Accuracy	Mean Distance	Maximum Distance	Standard Deviation
2	96.95%	7.69	17.64	3.88
4	98.55%	3.22	8.13	1.94
6	99.40%	1.52	2.94	0.6
8	99.74%	0.48	0.99	0.18

3.4 Test Validation

In order to validate the hypothesis on sampling points we proposed, other 8 female models are included in this study. For these 8 scanned models, the number of sampling points were decided by the length of chest circumference, and all of acceptable results can be achieved with limited harmonics in practice. Fig.5 demonstrates the imitations and Table 3 represents the error metrics.

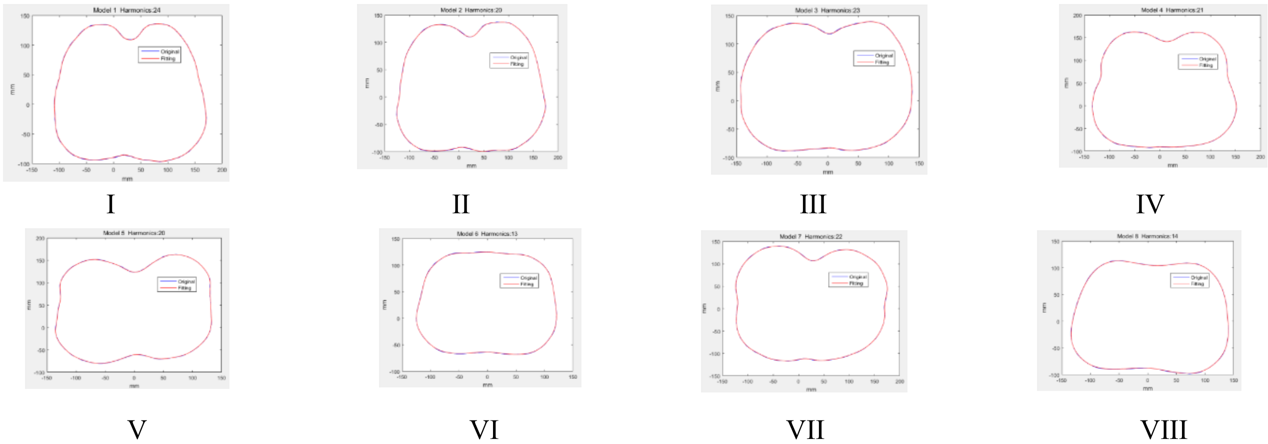

Fig.5 Construction result of other 8 scanned model. The number of sampling points is based on the girth of chest contour and mean error.

Table.3 Error metrics of 8 scanned model. The measure unit of perimeter, mean distance and max distance is millimeter

Model	Perimeter	Sampling Points	Harmonics	Perimeter Accuracy	Mean Distance	Max Distance	Std.
I	880	1760	24	99.70%	0.29	0.99	0.16
II	917	1834	20	99.66%	0.34	0.95	0.2
III	868	1736	23	99.67%	0.3	0.98	0.19
IV	920	1840	21	99.70%	0.3	0.99	0.18
V	891	1782	20	99.67%	0.32	0.91	0.18
VI	738	1476	13	99.70%	0.32	0.93	0.17
VII	950	1900	22	99.70%	0.31	0.96	0.18
VIII	830	1660	14	99.72%	0.31	0.94	0.16

4. Conclusion

In this article, EFA was used as the basic technique to reconstruct the female chest contour. There are three factors which influence the fitting result, which is the sampling method, sampling density and harmonics number. First, in this study, equally spaced sampling is selected as the best one through our experiments. Second, to reduce variables in the fitting process, we proposed a facile hypothesis to decide the sampling interval based on the mean error and the girth of chest, meanwhile validated the availability of this method. After that, the last factor left is the number of harmonics and which was easy to decide according to the fitting result and error metrics. There may be other methods to decide the number of sampling points, however, in practice, the hypothesis we proposed here is effective for the Elliptic Fourier fitting of female chest contour with limited harmonics.

5. Acknowledgement

This work is supported by National Natural Science Foundation of China (Grant No.61572124) and Shanghai Natural Science Foundation (Grant No.14ZR1401100).

References

[1] Kuhi FP, Giardina CR. Elliptic Fourier features of a closed contour [J]. Computer Graphics and Image Processing: 1982; 18 (3): 236-258.

[2] Adebowale A, Nicholas A, Lamb J, et al. Elliptic Fourier analysis of leaf shape in southern African Strychnos section Densiflorae (Loganiaceae) [J]. Botanical Journal of the Linnean Society: 2012; 170 (4): 542-553.

[3] Neto JC, Meyer G , Jones DD, et al. Plant species identification using Elliptic Fourier leaf shape analysis [J]. Computers and Electronics in Agriculture: 2006; 50 (2): 121-134.

[4] Viscosi V, Fortini P. Leaf shape variation and differentiation in three sympatric white oak species revealed by elliptic Fourier analysis [J]. Nordic Journal of Botany: 2011; 29 (5): 632-640.

[5] Friess M, Rohlf FJ, Hsiao HW. Quantitative Assessment of Human Body Shape Using Fourier Analysis [M]//CORNER B D, LI P, PARGAS R P. Three-Dimensional Image Capture and Applications Vi. Bellingham: Spie-Int Soc Optical Engineering: 2004; 117-124.

[6] Liu H, Zhang M, Chen Ds, et al. Study on bust curve of standard female figure [J]. Journal of Textile Research: 2011; 32 (2): 117-120.

[7] Shang Xm, Lu C, Wang H. Human body circumference curve fitting model base on automatic measurement [J]. Journal of Textile Research: 2010; 31 (4): 128-131, 138.

[8] Abels A, Kruusmaa M. (2009). Design of a shape-changing anthropomorphic mannequin for tailoring applications. International Conference on Advanced Robotics (pp.1-6). IEEE.

[9] SlavenkaPetrakDubravkoRogale, (2006), "Systematic representation and application of a 3D computeraided garment construction method", International Journal of Clothing Science and Technology: Vol.18 Iss3 pp. 179 -187.

[10] Hu YF. (2009). The application of geomagic studio software in reverse engineering post-processing. Manufacturing Automation: 5 (5); 501-524.

[11] (1982). Elliptic Fourier Features of a Closed. Contour, Comp. Graphics Image Process.

[12] R N. Bracewell, The Fourier transform, Scientific American: 260 (1989); 62-69.

[13] Iwata H, Niikura S, Matsuura S, Takano Y, Ukai Y. Interaction between genetic effects and soil type in diallel analysis of root shape and size of Japanese radish (Raphaunussativus L), Breeding Science: 54 (2004); 313-385.

[14] Tracey SR, Lyle JM, Duhamelb G. Application of elliptical Fourier analysis of otolith form as a tool for stock identificationi, Fisheries Research: 77 (2006); 138-147.

[15] Rohlf FJ, Archie JW. Acomparison of Fourier methods for the description of wing shape in mosquitoes. (Riteraculicidae), Syst. Zool: 33 (1984); 302-317.

[16] Neto JC, Meyer GE, Jones DD, Samal AK. (2006). Plant species identification using elliptic fourier leaf shape analysis. Computers & Electronics in Agriculture: 50 (2); 121-134.

[17] Daegling DJ, Jungers WL. Elliptical Fourier analysis of symphyseal shape in great ape mandibles, J. Hum. Evol: 39; (1) (2000): 107-122.

[18] Granlund GH. Fourier Preprocessing for Hand Print Character Recognition, IEEE Trans. Comput: 21 (1972) 195-201.

[19] Wallace TP, Wintz PA. An efficient three-dimensional aircraft recognition algorithm using normalized fourier descriptors, Comput. Graph. Image Process: 13 (2) (1980); 99-126.

[20] Freeman H. 1974: Computer processing of line drawing images, Compute Survey: 6; 57-97.

[21] Sanfilippo PG, Grimm JL, Flanagan JG, Lathrop KL, Sigal IA. (2014). Application of elliptic fourier analysis to describe the lamina cribrosa shape with age and intraocular pressure. Experimental Eye Research: 128; 1-7.